

^{51}V solid-state NMR and density functional theory studies of eight-coordinate non-oxo vanadium complexes: oxidized amavadin

Kristopher J. Ooms,^a Stephanie E. Bolte,^a Bharat Baruah,^b Muhammad Aziz Choudhary,^{b,c} Debbie C. Crans^{*b} and Tatyana Polenova^{*a}

Received 14th November 2008, Accepted 10th February 2009

First published as an Advance Article on the web 13th March 2009

DOI: 10.1039/b820383k

Using ^{51}V magic angle spinning solid-state NMR spectroscopy and density functional theory calculations we have characterized the chemical shift and quadrupolar coupling parameters for two eight-coordinate vanadium complexes, $[\text{PPh}_4][\text{V}(\text{v})(\text{HIDPA})_2]$ and $[\text{PPh}_4][\text{V}(\text{v})(\text{HIDA})_2]$; HIDPA = 2,2'-(hydroxyimino)dipropionate and HIDA = 2,2'-(hydroxyimino)diacetate. The coordination geometry under examination is the less common non-oxo eight coordinate distorted dodecahedral geometry that has not been previously investigated by solid-state NMR spectroscopy. Both complexes were isolated by oxidizing their reduced forms: $[\text{V}(\text{iv})(\text{HIDPA})_2]^{2-}$ and $[\text{V}(\text{iv})(\text{HIDA})_2]^{2-}$. $\text{V}(\text{iv})(\text{HIDPA})_2^{2-}$ is also known as amavadin, a vanadium-containing natural product present in the *Amanita muscaria* mushroom and is responsible for vanadium accumulation in nature. The quadrupolar coupling constants, C_Q , are found to be moderate, 5.0–6.4 MHz while the chemical shift anisotropies are relatively small for vanadium complexes, –420 and –360 ppm. The isotropic chemical shifts in the solid state are –220 and –228 ppm for the two compounds, and near the chemical shifts observed in solution. Presumably this is a consequence of the combined effects of the increased coordination number and the absence of oxo groups. Density functional theory calculations of the electric field gradient parameters are in good agreement with the NMR results while the chemical shift parameters show some deviation from the experimental values. Future work on this unusual coordination geometry and a combined analysis by solid-state NMR and density functional theory should provide a better understanding of the correlations between experimental NMR parameters and the local structure of the vanadium centers.

Introduction

Vanadium has a diverse coordination chemistry and can be found routinely in environments with coordination numbers ranging from three to eight giving rise to many complexes that have useful chemical and biochemical properties.^{1,2} Even though vanadium is a trace element in biological systems, it is an essential co-factor in a number of enzymes, also acts as an insulin enhancing agent and has been found as a natural product in the mushroom *Amanita muscaria*.^{2–8} The biological activity of vanadium complexes and proteins is determined by the specific chemical environment of the vanadium centers. The application of ^{51}V NMR to study solid vanadium-containing complexes that are of biological relevance has grown rapidly in recent years^{9–25} due to the ability to acquire high quality magic angle spinning spectra of both the central and satellite NMR transitions of the ^{51}V ($I = 7/2$). Studies have demonstrated that both the quadrupolar coupling and the chemical shift anisotropy, which can be determined from the

solid-state NMR spectra, are sensitive to the local vanadium environment and can be used to understand changes in the local molecular orbital structure and ground state charge distribution at the vanadium.^{9–24} Therefore, it is important to determine the ^{51}V solid-state NMR parameters of less common coordination geometries in vanadium complexes.

In nature, one of the highest concentrations of vanadium can be found in the *Amanita muscaria* mushrooms.^{6,7} Vanadium levels as high as 400 mg kg⁻¹ of mushroom have been reported.⁷ The vanadium is found in the mushroom as an eight coordinate complex, amavadin (Fig. 1), in a highly distorted cubic geometry that does not include the common V=O bonds.^{26,27} While amavadin shows unique redox capabilities including peroxidative halogenation^{28,29} and oxygen activation,³⁰ its role in the biological processes of the *Amanita* mushroom is unknown. Information about the electronic properties of the vanadium center may be important for understanding the chemical properties and the function of this unusual molecule. Furthermore, it is known that the redox potential of the amavadin is different by 100 mV from that of the simpler analog, whereas electron transfer processes to the vanadium are indistinguishable.³¹

The structure of the vanadium in amavadin does not change dramatically upon oxidation. The oxidized amavadin complex and its analog thus offer a unique opportunity to study an eight coordinate vanadium geometry and to compare the effect that such coordination has on the electric field gradient (EFG)

^aDepartment of Chemistry and Biochemistry, 036 Brown Laboratories, University of Delaware Newark, Delaware 19716. E-mail: tpolenov@mail.chem.udel.edu; Fax: +302 831 6335; Tel: +302 831 1968

^bDepartment of Chemistry, Colorado State University, Fort Collins, CO 80523. E-mail: crans@lamar.colostate.edu; Fax: +970 491 1801; Tel: +970 491 7635

^cDepartment of Chemistry, The University of Azad Jammu & Kashmir, Muzaffarabad, 13100, Pakistan

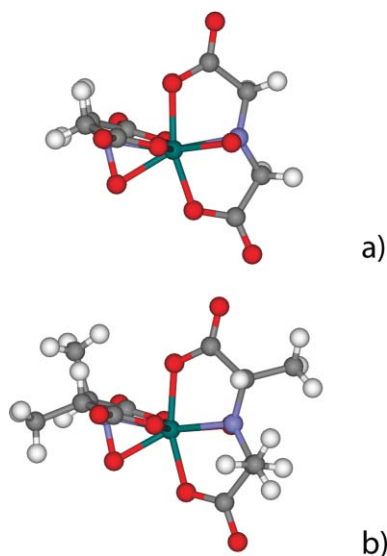


Fig. 1 The structure of (a) $[\text{PPh}_4][\text{V}(\text{v})(\text{HIDA})_2] \cdot \text{CH}_2\text{Cl}_2$ and (b) $[\text{PPh}_4][\text{V}(\text{v})(\text{HIDPA})_2] \cdot \text{H}_2\text{O}$. The structures were obtained from the Cambridge crystal structure database; depository names YAPHOM and YAPHUS, respectively. Hydrogen atoms are colour coded white, carbon atoms = grey, nitrogen atoms = blue, oxygen atoms = red, and vanadium atoms = green.

and chemical shift anisotropy (CSA) in the solid state. Recently, the role of each steric factor in the unique eight coordinate geometry of the amavadin complex has been explored using DFT calculations, structural analysis and solution ^{51}V chemical shifts.³² These studies revealed that the unusual deshielding of the ^{51}V resonances for amavadin and analogs can be attributed to a number of structural increments from regular substituent effects, and that the largest contribution arises from the non-oxo nature of these complexes.³² The variation that diastereomeric isomers had on the chemical shifts was considered to be minor. In this study, we present ^{51}V solid-state NMR spectra of the oxidized form of the natural product amavadin, $(\text{PPh}_4)[\text{V}(\text{v})(\text{HIDPA})_2]$, and one of its analogs, $(\text{PPh}_4)[\text{V}(\text{v})(\text{HIDA})_2]$; HIDPA and HIDA stand for the basic forms of 2,2'-(hydroxyimino)dipropionate and 2,2'-(hydroxyimino)diacetate, respectively. The NMR parameters for the two compounds are discussed in terms of coordination environment and compared to the current body of ^{51}V solid-state NMR data for other vanadium complexes. Surprisingly, the results reveal moderate quadrupolar coupling constants and small chemical shift anisotropies for both oxidized amavadin and its analog indicative of symmetric electronic charge distribution at the vanadium center. The DFT calculations predict accurately the electric field gradient tensor whereas the computed chemical shift anisotropy tensors show discrepancies with the experiment suggesting unusual electronic environment in these rare eight-coordinate non-oxo vanadium complexes.

Results and discussion

^{51}V solid-state NMR parameters

The NMR spectra of the two eight-coordinate complexes acquired at 14.1 T and three magic angle spinning (MAS) frequencies are shown in Fig. 2. The spectra are typical of vanadium coordination

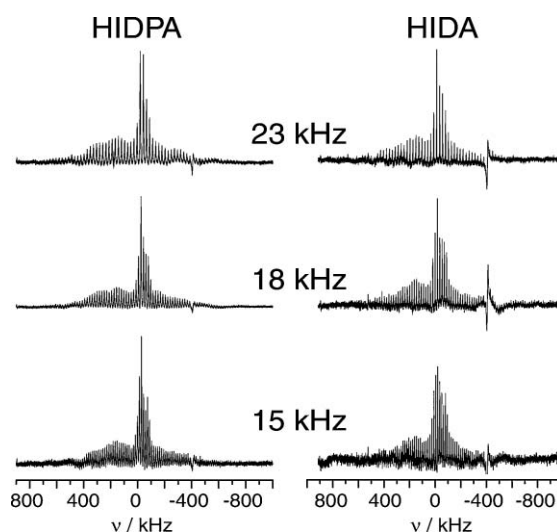


Fig. 2 Solid-state ^{51}V NMR spectra of the two complexes obtained at 14.1 T and different MAS rates. The signal observed at -600 kHz is from the copper coil.

complexes and contain NMR signal from both the central and satellite transitions. Using SIMPSON,³³ numerical simulations of the spectra were performed, and the ^{51}V chemical shift and quadrupolar coupling parameters were extracted, Table 1. The high quality of the fits is illustrated in Fig. 3 using the spectra for HIDA and HIDPA complexes acquired with the MAS frequency of 18 kHz. The isotropic chemical shift in the HIDA complex, $\delta_{\text{iso}} = -220$ ppm while in HIDPA $\delta_{\text{iso}} = -268$ ppm. These values are significantly less shielded than those observed for seven-coordinate complexes, where the isotropic shifts typically ranged from -570 to -680 ppm. Similarly, in solution the ^{51}V resonances for the oxidized amavadin complex and its analog are reported to be significantly less shielded than in the corresponding six- and seven-coordinate complexes. Specifically, the oxidized form of amavadin, $[\text{V}(\text{v})(\text{HIDPA})_2]^-$, showed chemical shifts ranging from -281 ppm³⁴ to -252 ppm,³⁵ and for the analog, $[\text{V}(\text{v})(\text{HIDA})_2]^-$ the corresponding shift was -263 ppm.³⁶ Therefore, these compounds exhibit unusual chemical shifts both in solution and in the solid state, and this behaviour has been attributed to the unique geometric and electronic structure of these complexes.

Smaller isotropic shifts observed for $[\text{V}(\text{v})(\text{HIDPA})_2]^-$ and $[\text{V}(\text{v})(\text{HIDA})_2]^-$ suggest that on average the mixing between the high energy occupied and low energy unoccupied molecular orbitals is better in these eight coordinate complexes than in complexes with lower coordination numbers.³⁷ The anisotropy of the chemical shift is also smaller than that observed typically in seven coordinate complexes, and resembles more the anisotropy of a five- or six-coordinate complex. The smaller anisotropy indicates that the magnitude of the vanadium shielding is similar in all directions, suggesting a relatively symmetric molecular orbital environment at the vanadium atom. Given the fact that these complexes contain no $\text{V}=\text{O}$ groups, the high symmetry at the distorted cubic vanadium atoms can be readily reconciled.

To rationalize the detected moderate quadrupolar coupling constant, the electronic charge distribution at the vanadium site needs to be analyzed. Based on simple point charge models, vanadium in a site of cubic symmetry will experience no electric

Table 1 Experimental and calculated ^{51}V solid-state NMR parameters for the eight coordinate non-oxo amavadin-type vanadium(v) complexes

Compound	Method (geometry)	C_Q/MHz	η_Q	$\delta_{\text{iso}}/\text{ppm}$	δ_σ/ppm	η_σ	$\alpha/\beta/\gamma$	
HIDA	Experiment	5.0 ± 0.1	0.2 ± 0.1	-220 ± 5	-420 ± 20	0.5 ± 0.05	$-45/0/90$	
	b3lyp/6-311 + G(d,p) (X-ray)	-4.38	1.0	-615	-131	0.426		
	b3lyp/6-311 + G(d,p) (optimized)	5.42	0.89	-561	-131	0.03		
	b3lyp/6-311 + G(d,p)	5.27	0.91	-557	-136	0.04		
	b3lyp/6-311++G	4.59	0.99	-611	-136	0.04		
	b3lyp/tzvp	-3.51	0.65	-577	-141	0.03		
	PBE1PBE/6-311 + G(d,p)	5.34	0.89	-609	-115	0.02		
	PBE1PBE/6-311++G	4.66	0.96	-673	-115	0.02		
	PBE1PBE/tzvp	-3.41	0.64	-638	-120	0.02		
	PBEPBE/6-311 + G(d,p)	-4.48	0.93	-340	245	0.08		
	PBEPBE/6-311++G	-4.02	0.85	-363	246	0.08		
	PBEPBE/tzvp	-2.96	0.34	-354	245	0.09		
	HIDPA	Experiment	6.4 ± 0.2	0.45 ± 0.1	-268 ± 0.1	-360 ± 8	0.5 ± 0.1	$90/0/90$
		b3lyp/6-311 + G(d,p) (X-ray)	-6.03	0.49	-630	-102	0.47	
b3lyp/6-311 + G(d,p) (optimized)		7.33	0.45	-572	-103	0.03		
b3lyp/6-311 + G(d,p)		7.20	0.46	-573	-109	0.03		
b3lyp/6-311++G		6.53	0.49	-630	-108	0.03		
b3lyp/tzvp		4.63	0.55	-591	-114	0.03		
PBE1PBE/6-311 + G(d,p)		7.25	0.45	-628	-85	0.03		
PBE1PBE/6-311++G		6.44	0.49	-695	-85	0.02		
PBE1PBE/tzvp		4.47	0.57	-655	-90	0.04		
PBEPBE/6-311 + G(d,p)		6.00	0.53	-353	251	0.07		
PBEPBE/6-311++G		5.27	0.59	-376	254	0.07		
PBEPBE/tzvp		3.46	0.72	-364	257	0.07		

(1) The chemical shift parameters are defined such that $|\delta_{zz} - \delta_{\text{iso}}| \geq |\delta_{xx} - \delta_{\text{iso}}| \geq |\delta_{yy} - \delta_{\text{iso}}|$, $\delta_{\text{iso}} = (\delta_{zz} + \delta_{yy} + \delta_{xx})/3$, $\delta_\sigma = \delta_{zz} - \delta_{\text{iso}}$, and $\eta_\sigma = (\delta_{yy} - \delta_{xx})/\delta_\sigma$. The components of the chemical shift tensor are $\delta_{ii} = (v_{ii} - v_{\text{ref}})/v_{\text{ref}}$. (ii = zz, xx, yy). (2) The EFG parameters are $C_Q = eQV_{zz}/h$ and $\eta_Q = (V_{xx} - V_{yy})/V_{zz}$ where $|V_{zz}| \geq |V_{yy}| \geq |V_{xx}|$, e is the electron charge and h is Planck's constant.

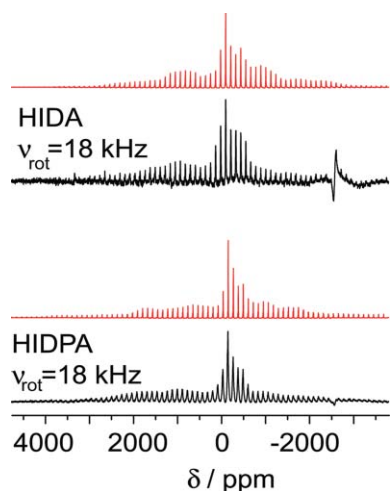


Fig. 3 Experimental (black) and simulated (red) spectra of the two complexes obtained while spinning the samples at 18 kHz at 14.1 T.

field gradient. However, when the ideal symmetry is broken an electric field gradient will be created at the vanadium site. The magnitude of these changes correlates directly to the magnitude of the electric field gradient and therefore, to the measured quadrupolar interaction parameters. Based on the NMR spectra it is determined that the quadrupolar coupling constants for the HIDA and HIDPA complexes are 5.0 and 6.4 MHz, respectively. The asymmetry parameters of the EFG tensor are 0.2 and 0.45 for the HIDA and HIDPA, respectively. These values can be considered average in size; typically the ^{51}V C_Q values for coordination complexes studied to date range from *ca.* 3 MHz to as high as 8.3 MHz. Therefore, it can be concluded that despite

the high coordination number, the distribution of charge in the vicinity of the vanadium atom deviates from spherical symmetry.

In addition to the chemical shift and EFG tensor parameters, the Euler angles that define the relative orientation of the two tensors can be found by fitting the spinning side bands envelope of the satellite transitions. Due to the low signal-to-noise ratio in the outer satellites as well as the lack of well-defined features in the envelope the error on the angles is large. Despite this, it is clear that β is close to 0° in both complexes, placing V_{zz} along δ_{zz} ; the angles used in the simulations are listed in Table 1.

DFT calculations of the NMR parameters

Quantum chemical calculations of ^{51}V NMR parameters have provided a valuable link between experimental NMR observables and the structure of vanadium complexes.^{17,18,23,24,32,38-42} Table 1 contains the results of calculations performed on the HIDA and HIDPA complexes using three functionals, b3lyp, PBE1PBE, and PBEPBE, and three basis sets, 6-311++G(d,p), 6-311++G, and tzvp as available in the Gaussian03 program.⁴³ The results obtained for the quadrupolar coupling constant and the asymmetry parameters of the EFG tensor for the HIDPA complex are in good agreement with experiment. The C_Q calculated for the HIDA complex is also well reproduced while the η_Q parameter shows a greater deviation from experiment. Calculations using b3lyp and PBE1PBE functionals and 6-311++G(d,p) or 6-311++G basis sets yield good agreement with experiment while calculations performed with PBEPBE functional (all basis sets) and those using a tzvp basis set (all functionals) underestimate the C_Q . All calculations were performed using a single molecule without the inclusion of counterions. Given the good agreement of the EFG calculations with the experiment, we conclude that the

EFG at the vanadium is almost completely determined by the vanadium complex. Longer-range influences from counterions and neighbouring complexes are negligible and need not be considered further.

Unlike the EFG calculations, the calculated magnetic shieldings (where the shieldings have been converted to chemical shifts as described in the methods section) show greater deviations from the experimental values. The calculated δ_{iso} values are significantly more shielded than the experimental results while the calculated anisotropies of the tensor are smaller than the experimental values. The worst agreement between experiment and theory is reached when PBEPBE functional is used: the sign of the chemical shift anisotropy is incorrect (Table 1). Further analysis of the computational results reveals that the largest discrepancies arise from the δ_{xx} and δ_{yy} components of the tensor, both of which are much more shielded than experimentally observed. To understand the possible source of the error we assume that the calculated orientation of the EFG in the molecular frame is correct; this is a good assumption given the success of the EFG calculation. Using our experimental Euler angles we note that δ_{zz} should be parallel to V_{zz} , *i.e.* $\beta = 0^\circ$. According to the calculations, V_{zz} is oriented along the approximate N–V–N axis, see Fig. 4. The shielding along this axis, δ_{zz} , is dictated by the molecular orbitals in the perpendicular plane. In the case of HIDA, this plane consists mostly of bonds between the vanadium and the carboxy oxygen atoms. Conversely, the δ_{xx} and δ_{yy} components of the chemical shift tensor contain contributions from the oxyamine portion of the ligands. Since it is δ_{xx} and δ_{yy} that are reproduced less well in the calculations, it is likely that it is the coordination of the oxyamines to the vanadium that is the source of the discrepancies in the calculations. Similar behavior was reported in a previous study of vanadium complexes with oxyamine ligands where substantial errors were observed for δ_{zz} , the chemical shift component perpendicular to the oxyamine plane.^{24,32} The fact that even at this level of theory difficulties are encountered in describing the interaction between the three-membered oxyamine-vanadium is consistent with the well-known problems with calculations of these strained compounds. The lower calculated anisotropies suggest that the molecule is less symmetric than the models used and indicate that the calculations underestimate the bonding between the vanadium and the oxyamine unit when using the X-ray structures.

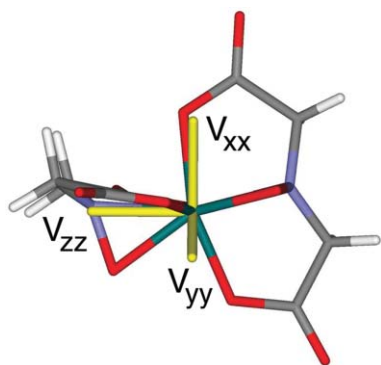


Fig. 4 The orientation of the EFG tensor with respect to the HIDA complex as determined by the DFT calculations. Hydrogen atoms are color coded white, carbon atoms = grey, nitrogen atoms = blue, oxygen atoms = red, and vanadium atoms = green.

Interpreting ^{51}V NMR parameters in terms of molecular structure

From an NMR and chemistry perspective, the results for the non-oxo eight-coordinate oxidized amavadin-type complexes presented here provide a key data set that allows us to expand our understanding of the dependence of the ^{51}V anisotropic solid-state NMR parameters on the vanadium coordination environment. These studies are the first in which vanadium compounds lacking a V=O group and exhibiting eight-coordination geometry are investigated by solid-state NMR, and thus will test the possibility that NMR can assist chemists in the characterization and identification of new vanadium-containing compounds. For the ^{51}V NMR to be used as a predictive tool, typically the NMR parameters for related series of compounds are compiled into a database, and empirically observed trends are subsequently used for building structural models for new compounds. In order to establish such correlations between ^{51}V NMR parameters and chemical structures a wide range of vanadium compounds of different coordination geometries and ligand sets has to be investigated. We have started building such a database using ^{51}V solid-state NMR to characterize vanadium(v) in an extensive range of chemical and geometric environments from various classes of compounds and with different coordination geometries,^{17,23,24} and can therefore examine the current results together with those from our prior work. The most fundamental correlations that are often made are those between the chemical shift anisotropy (or the isotropic chemical shift), or the C_Q , and the coordination number of the atom of interest. For example, such correlations for ^{29}Si have provided a valuable method for characterizing the local environment of different silicon atoms in a range of silicate materials; similarly correlations for aluminum have been observed.⁴⁴ Additionally, geometric factors such as bond angle and length often produce trends in the NMR parameters such as those observed for ^{17}O in glasses and ^{31}P in phosphates.^{45,46} The situation becomes more complex for transition metals which can have a wider range of geometries and coordination numbers, but some trends have also been suggested such as for ^{139}La coordination complexes and even ^{51}V in inorganic vanadia compounds.^{47,48}

In solution state a number of correlations between isotropic chemical shifts and coordination geometry have been reported for various vanadium complexes, although the empirical relationships are typically observed within classes of related molecules.^{1,9,49–51} For example, the chemical shifts of oxovanadates generally follow the degree of polymerization with the systematic changes in the ^{51}V shifts between monomer, dimer, tetramer, and pentamer.¹ Similarly, the chemical shifts for oxovanadium(v) complexes with diethanolamine and derivatives follow a pattern that varies with the substitutions on the diethanolamine.^{49,50} Chemical shift changes for vanadium alkoxides have been observed to vary with the steric bulk of alkoxides, and are found to be indicative of the coordination number of the vanadium.⁹ Solution studies of peroxovanadium(v)¹ and hydroxylamine^{1,51} complexes have demonstrated that both of these classes of compounds are significantly different from the more common six-coordinate coordination complexes and are akin to molecules investigated in this work.

All of the above correlations in the solid state and in solution are typically established in a series of related compounds or in materials where the identity of the coordinating atoms or ligands

is preserved, and only geometric-structural changes occur. In an attempt to decipher possible empirical correlations between the ^{51}V solid-state NMR parameters and the molecular structure features we have analyzed the aggregate of solid-state NMR data that we have generated in this work and in our several prior studies.^{17,23,24} These studies span a broad range of bioinorganic vanadium(v) complexes with different coordination numbers and different ligand sets, and thus represent the existing information available without any attempt to divide the molecules into the different classes of complexes.

Fig. 5 shows a plot of a derived quadrupolar parameter vs. the coordination number for a majority of the vanadium complexes for which ^{51}V solid-state NMR data are available.^{9,17,23–25,52,53} The derived quadrupolar parameter, $C_Q\sqrt{1-\eta^2/3}$, takes into account the asymmetry parameter of the EFG tensor as well as C_Q and is useful because it can be extracted based solely on the second-order quadrupolar shift.⁹ Perhaps not surprisingly, there is no clear trend in these graphs that would provide a useful correlation between the NMR observables and coordination number. For the quadrupolar coupling, the lowest values are observed for four and six coordinate complexes. This is likely the result of the fact that vanadium coordination geometry is close to tetrahedral and octahedral in these complexes. However, quadrupolar parameters close to 7 and 8 MHz can also be observed for four and eight coordinate vanadium, similar magnitudes as seen for the other coordination numbers. Clearly, the ability of vanadium to form non-ideal coordination geometries leads to a wide range of quadrupolar values.

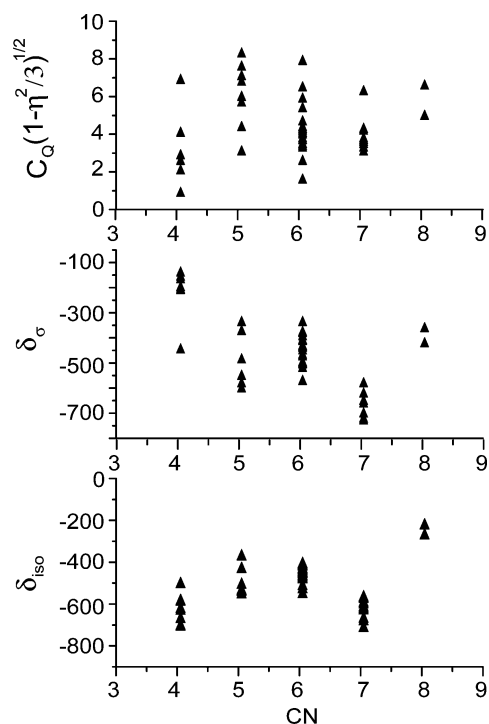


Fig. 5 Plots of the NMR parameters as a function of the vanadium coordination number (CN).

Fig. 5 also shows the chemical shift parameters, δ_σ and δ_{iso} , vs. the coordination number. Interestingly, these graphs show more clustering as a function of the coordination number. The chemical

shift anisotropy, δ_σ , decreases systematically as coordination number increases; excluding the eight coordinate complexes. This would be consistent with what has been reported for vanadia-based inorganic solids, where it has been observed that typically six-coordinate vanadium has larger chemical shift anisotropies than the four-coordinate species.⁴⁷ The trend is broken by the eight-coordinate complexes studied here, and may reflect the fact that the electronic and geometric environments are different from those in most compounds studied previously. Alternatively, the current findings might indicate that the bonding environment in the vicinity of the vanadium is better described as six-coordinate, *i.e.*, the oxyamine fragment should be treated as a single coordination position, an argument also put forth previously in the literature for oxyamine-type complexes.⁵¹ While clustering of the δ_{iso} values is also present, there is no linear trend in δ_{iso} as a function of coordination number. The results suggest that for vanadium δ_σ , and not δ_{iso} , is the more useful measure of the vanadium local structure, as has been observed previously.^{17,18,24}

Given the spread in the NMR parameter database as a function of coordination number, it is desirable that calculations be obtained as a link between the experimental parameters and the local structure in the vicinity of the vanadium. As has been shown above and in previous studies, DFT calculations of NMR parameters can be reasonably accurate when standard basis sets and functionals are used. Fig. 6 shows a plot of experimental C_Q and δ_{ii} ($\text{ii} = xx, yy, zz$) values for all the complexes that we have addressed previously by solid-state NMR and DFT calculations; calculations were performed using b3lyp functional and 6-311 + G** or 6-311 + G basis sets in Gaussian.^{17,23,24} From these plots it is evident that good agreement can be achieved between experiment and calculation. Typically the C_Q is predicted to within 15% of the experimental values, while the δ_{ii} values are underestimated by 50 to 200 ppm. It is interesting that for the chemical shift calculations the errors seem to be systematic. It has been previously reported that the typical agreements between experimental results and

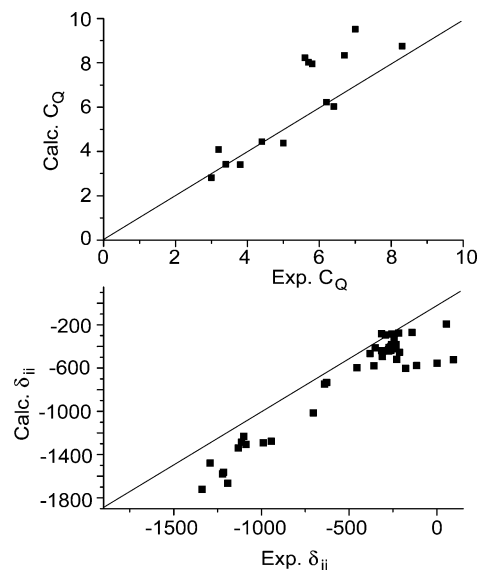


Fig. 6 Plots of the experimental vs. calculated NMR parameters for all vanadium(v) complexes studied by solid-state NMR and DFT computational methods. The solid lines represent perfect agreement between calculation and experiment.

theoretical chemical shift predictions are of the order of 100 ppm for ^{51}V .^{23,39} Previous investigations using different levels of theory have also revealed that, after a certain threshold, larger basis sets did not significantly improve the chemical shift parameters.²³ This suggests that the systematic deviation either arises from a fundamental ill representation in the calculations of a particular structural unit, or from a systematic issue in the atom positions obtained from single crystal X-ray diffraction. The relatively low resolution of the X-ray structure of amavadin complexes³⁴ may be one possible source of the discrepancy between the experimental and calculated shieldings. However, the rigidity of the ligand leaves little room for changes in the geometry of this complex. Indeed, DFT calculations using geometry-optimized structures have not improved the accuracy of the computed shieldings (Table 1). The possibility that some of the error is due to the calculated shielding of the reference compound VOCl_3 , should also be considered, although this error is not expected to account for all of the observed discrepancies. Combined these results provide important benchmark data for which the analysis using both theory and experiment can be developed for future applications.

Experimental

Materials and methods

Vanadyl acetylacetonate, $[\text{VO}(\text{acac})_2]$ (99.99%), 2-bromopropionic acid ($\geq 99\%$), bromoacetic acid ($\geq 99\%$), tetraphenylphosphonium chloride (98%), zinc acetate dihydrate (98%) and Dowex HCR-W2 strong acid resin were purchased from Sigma-Aldrich. Sodium hydroxide, hydrochloric acid, ceric ammonium nitrate ($[\text{NH}_4]_2[\text{Ce}(\text{NO}_3)_6]$, 98%) and hydroxylamine hydrochloride ($\text{NH}_2\text{OH}\cdot\text{HCl}$, 98%) were purchased from Fisher Scientific. All compounds were used as received, and distilled deionized water was used in all syntheses. The ligands $\text{HIDPA} = 2,2'$ -(hydroxyimino)dipropionate and $\text{HIDA} = 2,2'$ -(hydroxyimino)diacetate and corresponding vanadium(IV) and vanadium(V) complexes were prepared with slight modifications of the reported syntheses.^{34,35,54–58}

Ligand synthesis: $\text{HIDA} = 2,2'$ -(hydroxyimino)diacetate. Hydroxylamine hydrochloride (3.47 g, 0.05 mol) was neutralized with 10 mL of 5.0 M NaOH. Bromoacetic acid (13.90 g, 0.10 mol) was slowly neutralized with 20 mL of 5.0 M NaOH maintaining the solution temperature at or below 0 °C. The hydroxylamine solution was then chilled to ~ 0 °C in a salt–ice bath. The bromoacetic acid solution was then added dropwise to the hydroxylamine solution, and care was taken to maintain the solution mixture at 0 °C. An additional 20 mL of 5.0 M NaOH were slowly added to the mixture, which was then allowed to stand for ~ 72 h in a refrigerator (-4 °C).

The mixture was then acidified to pH 4.0 with 1.0 M HCl. To this solution zinc acetate dihydrate (11.0 g, 0.0684 mol) was added. The mixture was allowed to stand overnight at ambient temperature. The resulting zinc complex was then filtered off, washed with 10 mL of ice-cold water and dried over P_2O_5 .

The zinc complex (3.0 g, 0.014 mol) obtained as described above was dissolved in 25 mL of water by dropwise addition of concentrated HCl until the solution was clear. This solution was loaded onto an acidic Dowex HCR-W2 cation exchange resin (column size 2.5 cm \times 30 cm) and eluted with 0.2 M NaOH. The

fraction containing the product was dried in a rotary evaporator at ambient temperature and then over P_2O_5 . The ^1H NMR spectra were similar to those reported previously.^{34,35,54–57}

$\text{HIPDA} = 2,2'$ -(hydroxyimino)dipropionate. HIPDA was synthesized using the above procedure except that 2-bromopropionic acid was employed in place of bromoacetic acid. The product was confirmed using ^1H NMR spectroscopy; this is a low yielding reaction ($< 10\%$ yield), and the material formed is less pure than in the reaction producing the HIDA ligand.

$[\text{Ca}(\text{H}_2\text{O})_5][\text{V}(\text{IV})(\text{HIDA})_2]\cdot\text{H}_2\text{O}$. The compound was prepared with $[\text{VO}(\text{acac})_2]$ (2.65 g, 10.0 mmol), HIDA (3.15 g, 21.1 mmol) and CaCl_2 (1.11 g, 10.0 mmol) in H_2O (100 mL). Blue prismatic crystals were obtained from H_2O –isopropyl alcohol using the slow liquid-diffusion technique at 293 K as described previously.⁵⁸

$[\text{Ca}(\text{H}_2\text{O})_5][\text{V}(\text{IV})(\text{HIPDA})_2]\cdot\text{H}_2\text{O}$. The compound was prepared following the above procedure for $[\text{Ca}(\text{H}_2\text{O})_5][\text{V}(\text{IV})(\text{HIDA})_2]\cdot\text{H}_2\text{O}$ except that HIPDA was used in place of HIDA . Blue crystalline product was obtained from H_2O –MeOH–isopropyl alcohol using the slow liquid-diffusion technique at 293 K as reported before.²⁷ This product was stable in the solid state and stored at -20 °C.

$[\text{PPh}_4][\text{V}(\text{V})(\text{HIDA})_2]\cdot\text{CH}_2\text{Cl}_2$. $[\text{Ca}(\text{H}_2\text{O})_5][\text{V}(\text{IV})(\text{HIDA})_2]\cdot\text{H}_2\text{O}$ was oxidized in H_2O by addition of one equivalent of $[\text{NH}_4]_2[\text{Ce}(\text{NO}_3)_6]$ following the reported synthesis.³⁴ The red $[\text{V}(\text{V})(\text{HIDA})_2]^-$ formed in solution was isolated by the addition to the CH_2Cl_2 solution of two equivalents of PPh_4Br . $[\text{PPh}_4][\text{V}(\text{V})(\text{HIDA})_2]$ thus formed was more soluble in the organic layer, which was separated from the aqueous layer using a separatory funnel. Solid product was isolated by evaporating CH_2Cl_2 , and the purity of the material was confirmed by NMR spectroscopy (^{51}V $\delta_{\text{iso}} = -263$ ppm).³⁴ The ^1H NMR spectra and elemental analysis showed that excess PPh_4Br was present in this sample. The solid-state NMR spectra were recorded within one month after preparation and before evidence for any sample decomposition.

$[\text{PPh}_4][\text{V}(\text{V})(\text{HIPDA})_2]\cdot\text{H}_2\text{O}$. $[\text{PPh}_4][\text{V}(\text{V})(\text{HIPDA})_2]$ was prepared using the procedure reported previously,³⁴ and the purity was determined by NMR spectroscopy.³⁴ This sample contained $< 5\%$ of an impurity that formed vanadate in solution, and the rest of the compound had the characteristic triplet–peak pattern with the central peak at ^{51}V $\delta_{\text{iso}} = -269$ ppm as reported previously for the samples containing $[\text{V}(\text{V})(\text{HIPDA})_2]^-$ with different stereoisomers.³⁴ The solid-state NMR spectra were recorded within one month after preparation and before evidence for any sample decomposition.

Solid-state NMR spectroscopy

Solid-state ^{51}V NMR spectra were acquired on a Tecmag Discovery spectrometer, interfaced with a wide bore 9.4 T Magnex magnet, and operating at a frequency of 105.23 MHz (9.4T) for ^{51}V . Spectra were also collected on a Varian InfinityPlus spectrometer operating at 157.61 MHz (14.1 T). Vanadium chemical shifts were referenced to neat VOCl_3 , $\delta_{\text{iso}} = 0.0$ ppm, used as an external reference.⁵⁹ This sample was also used to calibrate the 90° pulse widths, which were set to 4.0 μs ($\gamma B_1 / 2\pi \approx 62$ kHz)

and $3.2 \mu\text{s}$ ($\gamma B_1/2\pi \approx 76 \text{ kHz}$) at 9.4 and 14.1 T, respectively. The magic angle was set by maximizing the number of rotational echoes observed in the ^{23}Na NMR free induction decay of solid NaNO_3 . The angle was set for each sample; accurate setting of the MA is critical when acquiring spectra from the satellite transitions of quadrupolar nuclei over a broad frequency range.⁶⁰ A 4 mm Doty XC4 MAS probe was used for acquiring all the spectra at 9.4 T while a 3.2 mm Varian T3 MAS probe was used at 14.1 T. The temperature was 20 °C during all experiments and controlled to within ± 1 degree with a Varian VT controller. For each sample, spectra at several MAS frequencies were acquired. The MAS frequency was controlled by the Tecmag and Varian automated control units to within 5 Hz. All spectra were acquired using a one-pulse experiment with either 1 μs or 0.8 μs pulse, a spectral width of 2 MHz, and a recycle delay of 1 s. Proton decoupling did not significantly improve the spectra and was therefore not used. The NMR spectra were processed with Gaussian line broadening functions of 100 Hz, and baseline corrections. Spectra of the entire manifold of central and satellite transitions were simulated with SIMPSON,³³ using finite excitation pulses corresponding to the experimental conditions.

Computations

Gaussian03⁴³ was used to calculate the vanadium magnetic shielding and EFG tensors. The b3lyp,⁴³ PBE1PBE,^{61,62} and PBEPBE^{61,62} functionals were employed; for each method three basis sets were used for all atoms, the 6-311 + G(d,p), 6-311++G, and tzvp, as available in the Gaussian package. The coordinates utilized in the calculations were obtained from single-crystal X-ray diffraction data.³⁴ Carbon–hydrogen bond lengths were fixed as 1.09 Å in the non-optimized structures. An additional calculation of NMR parameters was performed for both compounds at the b3lyp/6-311 + G(d,p) level of theory with geometry-optimized structures at the same level of theory. The NMR parameters for reference VOCl_3 were calculated using geometry-optimized structures for each method. The calculated principal components of the magnetic shielding tensor, σ_{ii} ($i = 1, 2, \text{ or } 3$), were converted to the principal components of the chemical shift tensor, δ_{ii} , using the relation $\delta_{ii} = \sigma_{\text{iso}}(\text{ref.}) - \sigma_{ii}$, where $\sigma_{\text{iso}}(\text{ref.})$ is the calculated isotropic magnetic shielding of the geometry-optimized reference molecule VOCl_3 .

Conclusion

We have reported the first ^{51}V solid-state NMR spectra of eight-coordinate non-oxo vanadium complexes. The two complexes, the oxidized forms of amavadin and its analogue, show moderate quadrupolar couplings and chemical shift anisotropies. The isotropic chemical shifts are less shielded than in the other complexes reported and may reflect the lack of V=O group or the high coordination state. DFT calculations reproduce the experimental EFG parameters well while they reproduce poorly the chemical shifts relating to the oxyamine coordination to the vanadium. The fact that NMR parameters in solution and in the solid state are in close agreement suggests that the unusual coordination environments of these molecules are properly described experimentally. The origin of the discrepancy between theory and experiment for this unusual non-oxo coordination geometry is not understood at this time and needs future exploration.

Examination of the available data of solid-state NMR parameters for vanadium(v) complexes of different coordination geometries reveals no simple all-inclusive empirical trends between NMR parameters and coordination number. The overall success of the DFT calculations, however, provides a reliable link between experimental solid-state NMR and structure that makes ^{51}V solid-state NMR a valuable characterization method.

Acknowledgements

T. P. acknowledges financial support of the National Science Foundation (CHE-0750079) and the National Institutes of Health (P20-17716, COBRE individual sub-project). K. J. O. thanks the Natural Sciences and Engineering Research Council of Canada for financial support. D. C. C. acknowledges financial support of the Institute of General Medicine at the National Institutes of Health (GM40525) and the National Science Foundation (CHE-0628260 and CHE-0750079).

References

- 1 D. C. Crans, J. J. Smee, E. Gaidamauskas and L. Q. Yang, *Chem. Rev.*, 2004, **104**, 849–902.
- 2 D. Rehder, *Angew. Chem., Int. Ed. Engl.*, 1991, **30**, 148–167.
- 3 D. C. Crans, M. Mahroof-Tahir, M. D. Johnson, P. C. Wilkins, L. Q. Yang, K. Robbins, A. Johnson, J. A. Alfano, M. E. Godzala, L. T. Austin and G. R. Willsky, *Inorg. Chim. Acta*, 2003, **356**, 365–378.
- 4 D. C. Crans, L. Q. Yang, T. Jakusch and T. Kiss, *Inorg. Chem.*, 2000, **39**, 4409–4416.
- 5 D. Rehder, *Org. Biomol. Chem.*, 2008, **6**, 957–964.
- 6 D. Bertrand, *Bull. Soc. Chim. Biol.*, 1943, **25**, 194–197.
- 7 H. U. Meisch, W. Reinle and J. A. Schmitt, *Naturwissenschaften*, 1979, **66**, 620–621.
- 8 P. Buglyo, D. C. Crans, E. M. Nagy, R. L. Lindo, L. Q. Yang, J. J. Smee, W. Z. Jin, L. H. Chi, M. E. Godzala and G. R. Willsky, *Inorg. Chem.*, 2005, **44**, 5416–5427.
- 9 D. C. Crans, R. A. Felty, H. J. Chen, H. Eckert and N. Das, *Inorg. Chem.*, 1994, **33**, 2427–2438.
- 10 H. Eckert and I. E. Wachs, *J. Phys. Chem.*, 1989, **93**, 6796–6805.
- 11 S. Hayakawa, T. Yoko and S. Sakka, *Bull. Chem. Soc. Jpn.*, 1993, **66**, 3393–3400.
- 12 S. Hayakawa, T. Yoko and S. Sakka, *J. Solid State Chem.*, 1994, **112**, 329–339.
- 13 W. L. Huang, L. Todaro, L. C. Francesconi and T. Polenova, *J. Am. Chem. Soc.*, 2003, **125**, 5928–5938.
- 14 W. L. Huang, L. Todaro, G. P. A. Yap, R. Beer, L. C. Francesconi and T. Polenova, *J. Am. Chem. Soc.*, 2004, **126**, 11564–11573.
- 15 U. G. Nielsen, H. J. Jakobsen and J. Skibsted, *Inorg. Chem.*, 2000, **39**, 2135–2145.
- 16 U. G. Nielsen, H. J. Jakobsen and J. Skibsted, *J. Phys. Chem. B*, 2001, **105**, 420–429.
- 17 N. Pooransingh, E. Pomerantseva, M. Ebel, S. Jantzen, D. Rehder and T. Polenova, *Inorg. Chem.*, 2003, **42**, 1256–1266.
- 18 N. Pooransingh-Margolis, R. Renirie, Z. Hasan, R. Wever, A. J. Vega and T. Polenova, *J. Am. Chem. Soc.*, 2006, **128**, 5190–5208.
- 19 D. Rehder, T. Polenova and M. Buhl, *Annu. Rep. NMR Spectrosc.*, 2007, **62**, 50–116.
- 20 J. Skibsted, C. J. H. Jacobsen and H. J. Jakobsen, *Inorg. Chem.*, 1998, **37**, 3083–3092.
- 21 J. Skibsted, N. C. Nielsen, H. Bildsøe and H. J. Jakobsen, *Chem. Phys. Lett.*, 1992, **188**, 405–412.
- 22 J. Skibsted, N. C. Nielsen, H. Bildsøe and H. J. Jakobsen, *J. Am. Chem. Soc.*, 1993, **115**, 7351–7362.
- 23 S. E. Bolte, K. J. Ooms, B. Baruah, D. C. Crans, J. J. Smee and T. Polenova, *J. Chem. Phys.*, 2008, **128**, 052317/052311–052317/052311.
- 24 K. J. Ooms, S. E. Bolte, J. J. Smee, B. Baruah, D. C. Crans and T. Polenova, *Inorg. Chem.*, 2007, **46**, 9285–9293.
- 25 S. Nica, A. Buchholz, M. Rudolph, A. Schweitzer, M. Waechtler, H. Breitzke, G. Buntkowsky and W. Plass, *Eur. J. Inorg. Chem.*, 2008, 2350–2359.

- 26 E. Bayer and H. Kneifel, *Z. Naturforsch. Pt. B*, 1972, **B 27**, 207- &.
- 27 R. E. Berry, E. M. Armstrong, R. L. Beddoes, D. Collison, S. N. Ertok, M. Helliwell and C. D. Garner, *Angew. Chem., Int. Ed. Engl.*, 1999, **38**, 795–797.
- 28 P. M. Reis, J. A. L. Silva, J. da Silva and A. J. L. Pombeiro, *Chem. Commun.*, 2000, 1845–1846.
- 29 P. M. Reis, J. A. L. Silva, A. F. Palavra, J. da Silva, T. Kitamura, Y. Fujiwara and A. J. L. Pombeiro, *Angew. Chem., Int. Ed. Engl.*, 2003, **42**, 821–823.
- 30 M. V. Kirillova, M. L. Kuznetsov, J. A. L. Da Silva, M. F. C. Da Silva, J. Da Silva and A. J. L. Pombeiro, *Chem.–Eur. J.*, 2008, **14**, 1828–1842.
- 31 M. A. Nawi and T. L. Riechel, *Inorg. Chim. Acta*, 1987, **136**, 33–39.
- 32 K. R. Geethalakshmi, M. P. Waller and M. Buhl, *Inorg. Chem.*, 2007, **46**, 11297–11307.
- 33 M. Bak, J. T. Rasmussen and N. C. Nielsen, *J. Magn. Reson.*, 2000, **147**, 296–330.
- 34 E. M. Armstrong, R. L. Beddoes, L. J. Calviou, J. M. Charnock, D. Collison, N. Ertok, J. H. Naismith and C. D. Garner, *J. Am. Chem. Soc.*, 1993, **115**, 807–808.
- 35 J. Lenhardt, B. Baruah, D. C. Crans and M. D. Johnson, *Chem. Commun.*, 2006, 4641–4643.
- 36 J. M. Lenhardt, B. Baruah, D. C. Crans and M. D. Johnson, *Pure Appl. Chem.*, 2008, in press.
- 37 N. F. Ramsey, *Phys. Rev.*, 1950, **78**, 699–703.
- 38 M. Buhl, *J. Comput. Chem.*, 1999, **20**, 1254–1261.
- 39 M. Buhl and F. A. Hamprecht, *J. Comput. Chem.*, 1998, **19**, 113–122.
- 40 M. Buhl and M. Parrinello, *Chem.–Eur. J.*, 2001, **7**, 4487–4494.
- 41 M. Buhl, R. Schurhammer and P. Imhof, *J. Am. Chem. Soc.*, 2004, **126**, 3310–3320.
- 42 M. P. Waller, M. Buhl, K. R. Geethalakshmi, D. Wang and T. Walter, *Chem.–Eur. J.*, 2007, **13**, 4723–4732.
- 43 M. J. T. Frisch, G. W. Schlegel, H. B. Scuseria, G. E. Robb, M. A. Cheeseman, J. R. Montgomery, Jr., J. A. Vreven, T. Kudin, K. N. Burant, J. C. Millam, J. M. Iyengar, S. S. Tomasi, J. Barone, V. Mennucci, B. Cossi, M. Scalmani, G. Rega, N. Petersson, G. A. Nakatsuji, H. Hada, M. Ehara, M. Toyota, K. Fukuda, R. Hasegawa, J. Ishida, M. Nakajima, T. Honda, Y. Kitao, O. Nakai, H. Klene, M. Li, X. Knox, J. E. Hratchian, H. P. Cross, J. B. Bakken, V. Adamo, C. Jaramillo, J. Gomperts, R. Stratmann, R. E. Yazyev, O. Austin, A. J. Cammi, R. Pomelli, C. Ochterski, J. W. Ayala, P. Y. Morokuma, K. Voth, G. A. Salvador, P. Dannenberg, J. J. Zakrzewski, V. G. Dapprich, S. Daniels, A. D. Strain, M. C. Farkas, O. Malick, D. K. Rabuck, A. D. Raghavachari, K. Foresman, J. B. Ortiz, J. V. Cui, Q. Baboul, A. G. Clifford, S. Cioslowski, J. Stefanov, B. B. Liu, G. Liashenko, A. Piskorz, P. Komaromi, I. Martin, R. L. Fox, D. J. Keith, T. Al-Laham, M. A. Peng, C. Y. Nanayakkara, A. Challacombe, M. Gill, P. M. W. Johnson, B. Chen, W. Wong, M. W. Gonzalez, C and J. A. Pople, Gaussian, Inc., Wallingford, CT, Editon edn., 2004.
- 44 K. J. D. Mackenzie and M. E. Smith, *Multinuclear Solid-State NMR of Inorganic Materials*, Pergamon, Oxford, 2002.
- 45 T. M. Clark, P. J. Grandinetti, P. Florian and J. F. Stebbins, *Phys. Rev. B*, 2004, **70**, 0642021–0642028.
- 46 G. L. Turner, K. A. Smith, R. J. Kirkpatrick and E. Oldfield, *J. Magn. Reson.*, 1986, **70**, 408–415.
- 47 O. B. Lapina, V. M. Mastikhin, A. A. Shubin, V. N. Krasilnikov and K. I. Zamaraev, *Prog. Nucl. Magn. Reson. Spectrosc.*, 1992, **24**, 457–525.
- 48 M. J. Willans, K. W. Feindel, K. J. Ooms and R. E. Wasylshen, *Chem.–Eur. J.*, 2005, **12**, 159–168.
- 49 D. C. Crans, P. M. Ehde, P. K. Shin and L. Pettersson, *J. Am. Chem. Soc.*, 1991, **113**, 3728–3736.
- 50 D. C. Crans and P. K. Shin, *Inorg. Chem.*, 1988, **27**, 1797–1806.
- 51 A. D. Keramidis, S. M. Miller, O. P. Anderson and D. C. Crans, *J. Am. Chem. Soc.*, 1997, **119**, 8901–8915.
- 52 W. Basler, H. Lechert, K. Paulsen and D. Rehder, *J. Magn. Reson.*, 1981, **45**, 170–172.
- 53 L. Mafrá, F. A. Almeida Paz, F.-N. Shi, C. Fernandez, T. Trindade, J. Klinowski and J. Rocha, *Inorg. Chem. Commun.*, 2006, **9**, 34–38.
- 54 G. Anderegg, E. Koch and E. Bayer, *Inorg. Chim. Acta*, 1987, **127**, 183–188.
- 55 J. Felcman, M. Cândida, T. A. Vaz and J. J. R. Fraústo Da Silva, *Inorg. Chim. Acta*, 1984, **93**, 101–108.
- 56 E. Koch, H. Kneifel and E. Bayer, *Z. Naturforsch. B*, 1986, **41b**, 359–362.
- 57 P. D. Smith, S. M. Harben, R. L. Beddoes, M. Helliwell, D. Collison and C. D. Garner, *J. Chem. Soc., Dalton Trans.*, 1997, 685–691.
- 58 P. D. Smith, R. E. Berry, S. M. Harben, R. L. Beddoes, M. Helliwell, D. Collison and C. D. Garner, *J. Chem. Soc., Dalton Trans.*, 1997, 4509–4516.
- 59 R. K. Harris, E. D. Becker, S. M. C. De Menezes, R. Goodfellow and P. Granger, *Pure Appl. Chem.*, 2001, **73**, 1795–1818.
- 60 A. A. Shubin, O. B. Lapina and V. M. Bondareva, *Chem. Phys. Lett.*, 1999, **302**, 341–346.
- 61 J. P. Perdew, K. Burke and M. Ernzerhof, *Phys. Rev. Lett.*, 1996, **77**, 3865–3868.
- 62 J. P. Perdew, K. Burke and M. Ernzerhof, *Phys. Rev. Lett.*, 1997, **78**, 1396–1396.